QUASI-STATIC PRESSURE, DURATION, AND IMPULSE FOR EXPLOSIONS IN STRUCTURES

W. E. Baker
Charles E. Anderson, Jr.
Bruce L. Morris
Donna K. Wauters

Southwest Research Institute
6220 Culebra Road
San Antonio, Texas

ABSTRACT

Similitude analysis has been used to obtain dimensionless parameters for peak quasi-static pressures, blowdown duration, and specific impulse for blast loading within enclosures. Data from the United States and Europe have been collected and analyzed, and then displayed graphically according to relationships derived from the similitude analysis. Three graphs are presented, along with appropriate curve fits, of the peak quasi-static pressure versus the ratio of charge weight to enclosure volume, the reduced duration versus the reduced pressure, and the reduced specific impulse versus the reduced pressure.

NOMENCLATURE

A	= surface area of enclosure
F	= unit of force
L	= unit of length
T	= unit of time
V	= enclosure volume
W	= unit of energy
	= charge weight
a_o	= sound speed of air
c	= exponential decay constant
f	= functional relationship
g	= functional relationship
h	= functional relationship
i_g	= specific (gas) impulse
p	= pressure
p_o	= ambient pressure
p_{QS}	= peak gage quasi-static pressure
p_1	= peak absolute quasi-static pressure
t	= time

t_{max} = duration
α_{eff} = ratio of effective vent area to total enclosure surface area
γ = ratio of specific heats
π = nondimensional term
τ = nondimensional duration
σ = standard deviation

Superscripts:

- (bar) = nondimensional term
^ (carrot) = calculated quantity from curve fit

INTRODUCTION

The loading from an explosive charge detonated within a vented or unvented structure consists of two almost distinct phases. The first phase is that of reflected blast loading. It consists of the initial high pressure, short duration reflected wave, plus perhaps several later reflected pulses arriving at times closely approximated by twice the average time of arrival at the chamber walls. These later pulses are usually attenuated in amplitude because of irreversible thermodynamic process, and they may be very complex in waveform because of the complexity of the reflection process within the structure, whether vented or unvented. Maxima for the initial internal blast loads on a structure can be estimated from scaled blast data or theoretical analyses of normal blast wave reflection from a rigid wall. Following the initial and secondary shock wave reflections from the internal walls, the pressure settles to a slowly decaying level — the shock wave phase of the loading is over. The second phase of a slowly decaying pressure is a function of the volume and vent area of the structure, and the nature and energy release of the explosion.

The process of reflection and pressure buildup in either unvented or poorly vented structures has been recognized for some time, dating from World War II research on effects of bombs and explosives detonated within enclosures. However, very little data were available from WWII and no attempt was made to understand or relate the physical processes until 1968 when Weibull [1] correlated peak quasi-static pressure versus the charge weight for a series of experiments with TNT detonated within a vented enclosure. More recently, study of these pressures has revived because of interest in design of vented and unvented explosion containment chambers.

A typical time history of pressure at the wall of a vented structure is shown in Figure 1. One can see that the maximum quasi-static pressure is quite difficult to define because it is obscured by the initial shock and first few reflected shocks. Obviously, several reflections must occur before irreversible processes attenuate the shocks and convert their energy to quasi-static pressure. Therefore, it seems inappropriate to call point A in Figure 1 the peak quasi-static pressure, although this is the point used by Kingery, et al. [2] to compare with code predictions from Proctor and Filler [3] and

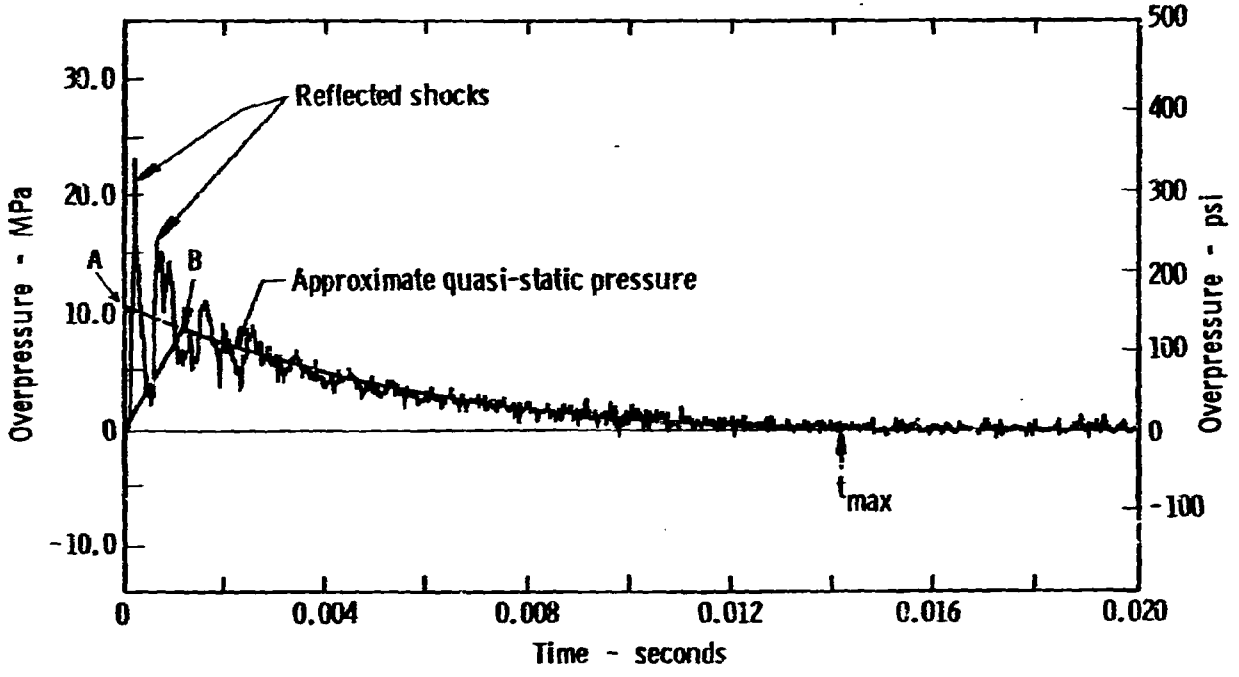

Figure 1. Typical Pressure-Time History of an Explosion in a Vented Structure

the Kinney and Sewell equation [4]. A better approach is to allow some time for establishing the maximum pressure, such as point B in Figure 1. The smaller the vent area to the total wall area, the closer the pressure at point B will be to that at point A, and in the limit of the vent area being zero (that is, an unvented enclosure), the pressures at points A and B will coincide.

Figure 1 also illustrates another problem inherent in reduction of vented pressure data: accurate determination of duration of this pressure. When the pressure approaches ambient, the shock reflections have largely decayed. But, the pressure approaches the baseline nearly asymptotically so that the duration is quite difficult to determine accurately. A possible duration t_{max} is shown in the figure.

In spite of complexities in the venting process, gas pressures and their durations can be predicted with reasonable accuracy, particularly if one differentiates between these relatively long term and low amplitude pressures from the internal blast pressures resulting from blast wave impingement and reflection. Generally of great interest in the blast loading of structures resulting from interior explosions are the peak quasi-static pressure, the duration, and the total impulse. The following paragraphs will develop and describe relationships among various physical parameters. Functional relationships will be derived from similitude analysis, but the exact functional form cannot be ascertained from this analysis without invoking restrictive, simplifying assumptions. However, a large quantity of experimental data, from a variety of sources [1-22], allow empirical relationships to be obtained.

SIMILITUDE ANALYSIS

A model analysis was performed to determine the functional form of the quasi-static pressure versus physical parameters pertinent to a vented structure. The problem is envisioned as an instantaneous energy release of magnitude W inside a confined volume V. A vent area (α_{eff} A) exists through which internal gases can escape, where α_{eff} is the effective ratio of vent area to total cross-sectional area of the walls. Ambient atmospheric pressure p_o exists initially inside and outside the confined volume. To define an equation-of-state for the gases in this problem requires two additional parameters which are the ratio of specific heats γ and speed of sound a_o. Table 1 summarizes the parameters in this problem and lists their fundamental dimensions in a system of units of force F, length L, and time T.

Nondimensional numbers, or pi terms, can be developed from the list of variables in Table 1. The assumptions in this analysis are all in the definition of the problem. Phenomena are not considered which do not have parameters listed in the table. Probably the major assumption invoked is that thermal effects are ignored — in other words, the pressures dissipate through venting and not through the conduction of heat into the walls of the structure. An acceptable set of pi terms which result are:

Table 1. Parameters Determining Quasi-Static Pressure Inside Vented Containment Vessel

Parameter	Symbol	Fundamental Dimensions	Reason for Including
Volume	V	L^3	Describe Geometry of Boundaries
Vented Area	$(\alpha_{eff} A)$	L^2	
Energy Release	W	FL	Input Energy
Atmospheric Pressure	p_o	F/L^2	Define the State of Air
Sound Speed in Air	a_o	L/T	
Specific Heat Ratio Air	γ	—	
Pressure Increase	p	F/L^2	Loading Functions
Time	t	T	
Impulse	i_g	FT/L^2	

$$\pi_1 = p/p_o \tag{1}$$

$$\pi_2 = \frac{(a_{eff}\, A)}{V^{2/3}} \tag{2}$$

$$\pi_3 = \gamma \tag{3}$$

$$\pi_4 = \frac{W}{p_o V} \tag{4}$$

$$\pi_5 = \frac{a_o\, t}{V^{1/3}} \tag{5}$$

$$\pi_6 = \frac{i_s}{p_o\, t} \tag{6}$$

Note, however, that π_6 adds no new information since the impulse can be explicitly obtained by integrating the pressure with respect to time.

In general terms, dimensional analysis states that the functional format for the reduced pressure, π_1, is given by:

$$\frac{p}{p_o} = f\left[\frac{W}{p_o V}, \frac{(a_{eff}\, A)}{V^{2/3}}, \gamma, \frac{a_o\, t}{V^{1/3}}\right] \tag{7}$$

If we are only interested in predicting the peak quasi-static pressure, the result will not depend upon time, hence the functional form must be invariant with respect to the last pi term. Likewise, for γ a constant (as it would be for air), the functional form will not depend upon γ, hence:

$$\bar{p} = f\left[\frac{W}{p_o V}, \frac{(a_{eff}\, A)}{V^{2/3}}\right] \tag{8}$$

where $\bar{p}$ is the ratio of the maximum absolute quasi-static pressure to ambient pressure, i.e.:

$$\bar{p} = \frac{p_{QS} + p_o}{p_o} \tag{9}$$

and p_{QS} is the conventional gage quasi-static pressure. Provided the flow through the vent is small relative to the rate of energy release, the maximum pressure will occur before significant venting has transpired. And since the ambient pressure is essentially an invariant, Equation (8) can then be written for the maximum quasi-static pressure:

$$p_{QS} = f\left[\frac{W}{V}\right] \tag{10}$$

The blow-down time, or duration, can also be expressed as a functional relationship with respect to the other pi terms:

$$\frac{t\, a_o}{V^{1/3}} = g\left[\frac{p}{p_o}, \frac{(a_{eff}\, A)}{V^{2/3}}, \gamma, \frac{W}{p_o\, V}\right] \tag{11}$$

But it just has been shown, if the maximum quasi-static pressure is reached before significant venting occurs, that the last term $W/(p_o V)$ is a function of the first term, p/p_o. And, since γ is an invariant, Equation (11) becomes:

$$\frac{t\, a_o}{V^{1/3}} = g\left[\frac{p}{p_o}, \frac{(a_{eff}\, A)}{V^{2/3}}\right] \tag{12}$$

Based on a theoretical analysis of chamber venting by Owczarek [22], Baker and Oldham [24] showed that

$$\frac{t\, a_o}{V^{1/3}} \propto \frac{V^{2/3}}{(a_{eff}\, A)} \tag{13}$$

or

$$t \propto \frac{V}{a_o\, (a_{eff}\, A)} \tag{14}$$

In physical terms, Expression (14) states that the blowdown time is directly proportional to the chamber volume divided by the effective venting area, not an unexpected result. Expression (13) thus allows us to simplify Equation (12) by defining a new scaled time $\bar{t}$:

$$\bar{\tau} = \left(\frac{t\, a_o}{V^{1/3}}\right)\left(\frac{a_{eff}\, A}{V^{2/3}}\right) = g\left[\frac{p}{p_o},\ 1\right] \tag{15}$$

$$\bar{\tau} = g\left[\frac{p}{p_o}\right] \tag{16}$$

Thus, the scaled duration is also only a function of the reduced pressure.

The last relationship to obtain is a nondimensional, or reduced, impulse $\bar{i}_g$. Figure 2 shows a simplified form for gas venting pressures. In this simplified form, the gas venting pressure is assumed to follow the solid curve which rises linearly from time zero until it reaches, at time t_1, a curve which is decaying exponentially from an initial maximum value of p_1, where p_1 is the absolute quasi-static pressure at time t = 0. The decay then follows the time history

$$p(t) = p_1\, e^{-ct} \tag{17}$$

until it reaches ambient pressure p_o at time $t = t_{max}$. The exponential decay is shown to agree well with experiment (Kingery, et al. [2], and Schumacher, et al. [5]). The cross-hatched area under the overpressure curve is defined as the gas impulse i_g, and is found by integrating Equation (17) with respect to time:

$$i_g = \int_o^{t_{max}} \left[p(t) - p_o\right] dt = \int_o^{t_{max}} \left(p_1\, e^{-ct} - p_o\right) dt$$

$$= \frac{p_1}{c}\left(1 - e^{-ct_{max}}\right) - p_o\, t_{max} \tag{18}$$

The duration, t_{max}, will be obtained from Equations (15) and (16). Likewise, as will be shown later, the exponential decay factor, c, can be written in terms of t_{max} and $\bar{p}$. As stated earlier, the impulse can thus be found explicitly from the other nondimensional relationships, but it is still useful to display the impulse graphically. Since the impulse depends upon the duration and the pressure, and the scaling factor for time is given by Expression (14), then a suitable choice of parameters to scale the impulse is:

$$\bar{i}_g = \frac{i_g\, a_o\, a_{eff}\, A}{p_o\, V} \tag{19}$$

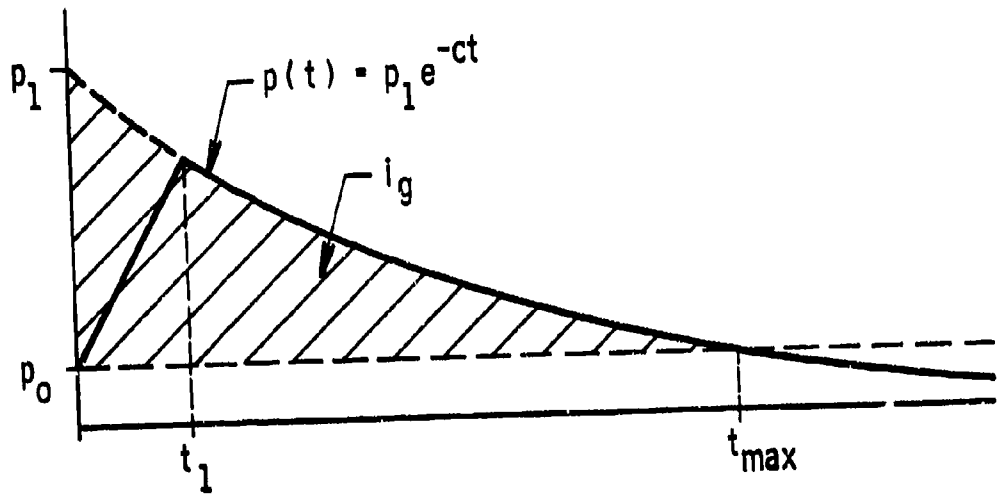

Figure 2. Simplified Pressure-Time History for Venting

But the maximum pressure and the scaled duration are functions only of the reduced pressure, hence

$$\bar{i}_g = h\left[\frac{p}{p_o}\right] \tag{20}$$

Equations (10), (16), and (20) express the functional relationships between the various physical parameters. The next section will empirically determine the functional forms via curve-fitting of experimental data. However, a brief discussion of the effective vent area ratio, α_{eff}, is in order.

Venting can be geometrically quite complicated for some structures, particularly those structures referred to as suppressive structures which often have three to six wall layers with various staggered venting patterns so fragments will not escape the confinement. For multi-walled confinement, an effective vent area ratio must be computed. To compute α_{eff} for a multi-walled structure, we have used

$$\frac{1}{\alpha_{eff}} \sum_{i=1}^{N} \frac{1}{\alpha_i} \tag{21}$$

where N is the number of elements in a suppressive structure panel. Although no proof of this relationship is presently possible, it does reach the appropriate limits for small and large numbers of plates. For example, if only one plate is present, $\alpha_{eff} = \alpha_1$ as it should. If an infinite number of plates is present, $\alpha_{eff} = 0$, with the flow completely choked. If one of the plates is solid, and thus has a zero α, $\alpha_{eff} = 0$ as it should. If all plates have the same value for α, $\alpha_{eff} = \alpha/N$, which is a number smaller than α for a single plate as would be expected. In each member, α is defined according to:

$$\alpha = \frac{A_{vent}}{A_{wall}} \tag{22}$$

For plates, the meaning of this definition is obvious. However, in angles and louvres, the definition is less obvious since angles and louvres are more efficient in constricting flow than are plates with holes. Details for computing the α's for more complicated geometries can be found in Baker and Oldham [24] and Baker, et al. [25].

GRAPHICAL DISPLAY OF DATA

The preceeding discussion determined which physical parameters are interrelated. This analysis permits the judicious choice of parameters to

display experimental data graphically. Equation (10) states that the peak quasi-static pressure is only a function of the charge energy-to-volume ratio. Thus, a plot of experimental data of p_{QS} versus W/V will determine this functional relationship. Figures 3 and 4 display the data from 177 tests, and as can be seen, the experimental data range over several orders of magnitude. Figure 3 is a graph of the data in metric units, while Figure 4 is the identical graph except it is displayed in English units. The data include tests conducted with the following high explosives (HE): TNT, PETN, PBX-9502, 50/50 Pentolite, dynamite, C-4, Comp B, and RDX.

One approximation has been made in plotting these data. For any given high explosive, the charge energy is directly proportional to the explosive mass. Also, the energy-to-mass ratio for most high explosives is approximately the same. Figures 3 and 4, for convenience, use the mass of the explosive for the symbol W. No attempt has been made to normalize all the high explosives to TNT since the scatter in data from experiments with the same high explosive often masks the effects of slight variations of the energy-to-mass ratio differences between explosives. (For carefully controlled experiments, the differences in effects of energy variation between explosives can be measured. Indeed, for a series of experiments conducted by Hokanson, et al. [21], where quasi-static pressures were measured for bare explosive and the same explosive mass encased in plastic and aluminum, the contribution of the oxidized casing to the peak quasi-static pressure was theoretically computed and measured experimentally.) It should be noted, however, that if explosion scenarios other than HE detonations are of interest, e.g., various fuel/air mixtures, then the TNT equivalent weight should first be determined and then used for W if these graphs are to be used to determine the peak quasi-static pressure.

It is reasonable to expect the peak quasi-static pressure to be directly proportional to the charge weight, and examination of the data in Figure 3 confirms this supposition for small and large W/V. For intermediate values of W/V, a transition region is evident. For $W/V < 0.4$ kg/m^3, complete oxidation of the explosive occurs. But if W/V is too large, insufficient oxygen is available to convert all the potential energy available in the explosive charge, and the energy release is reduced by the ratio of the heat of detonation to the heat of combustion. Thus, for $W/V > 11.0$ kg/m^3, the primary oxidizer available is that in the explosive itself. A transition region, $0.4 < W/V < 11.0$, connects the two regions. Linear least-squares curve fits have been performed on the data in the two end regions, and are shown in Figure 3.* A seventh-order polynomial of the form:

* All curve fittings in this article have been performed in log-log coordinates. Linear thus refers to the form of the curve in a log-log plot.

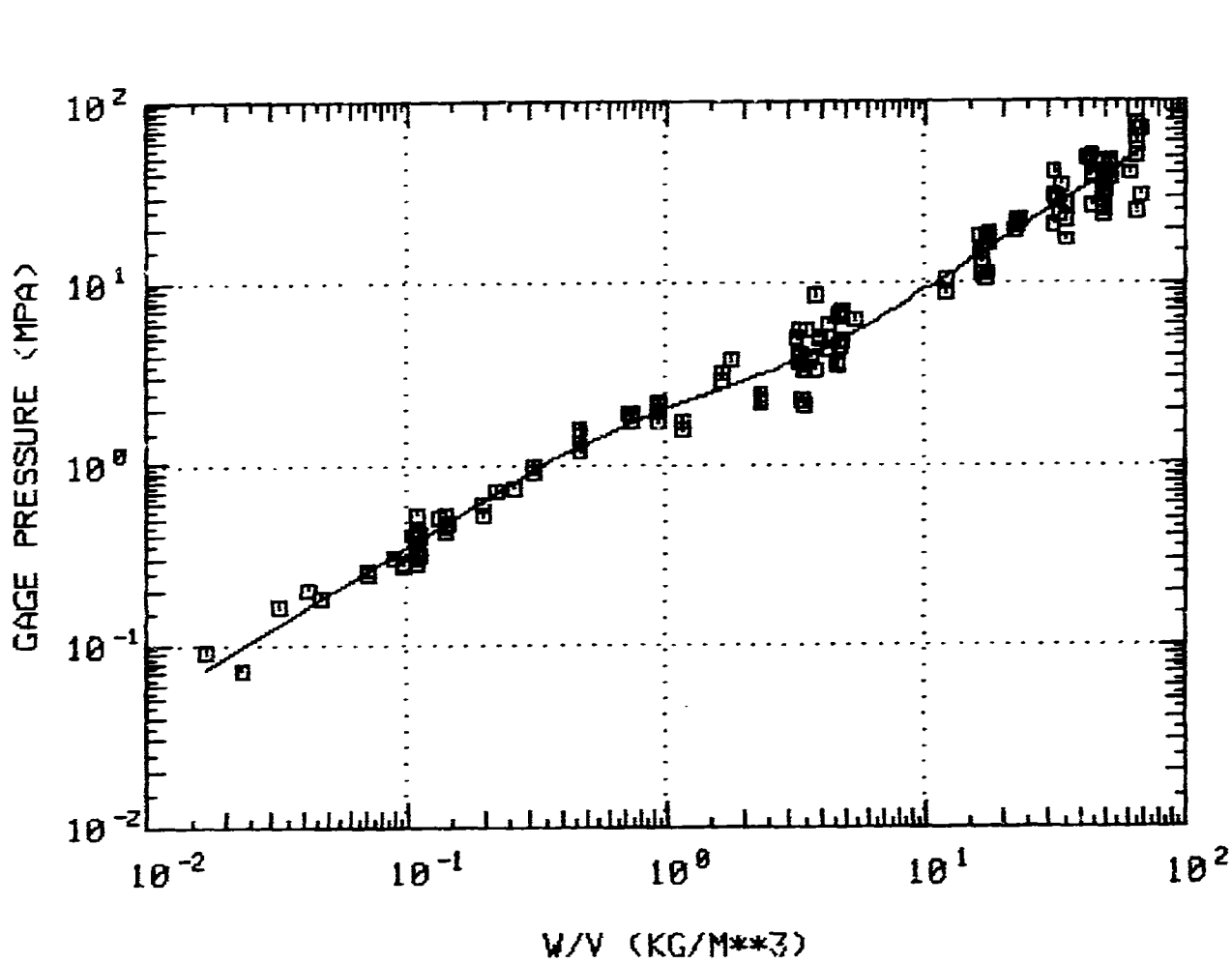

Figure 3. Peak Quasi-Static Pressure Versus the Ratio of Charge Weight to Enclosure Volume (Metric Units)

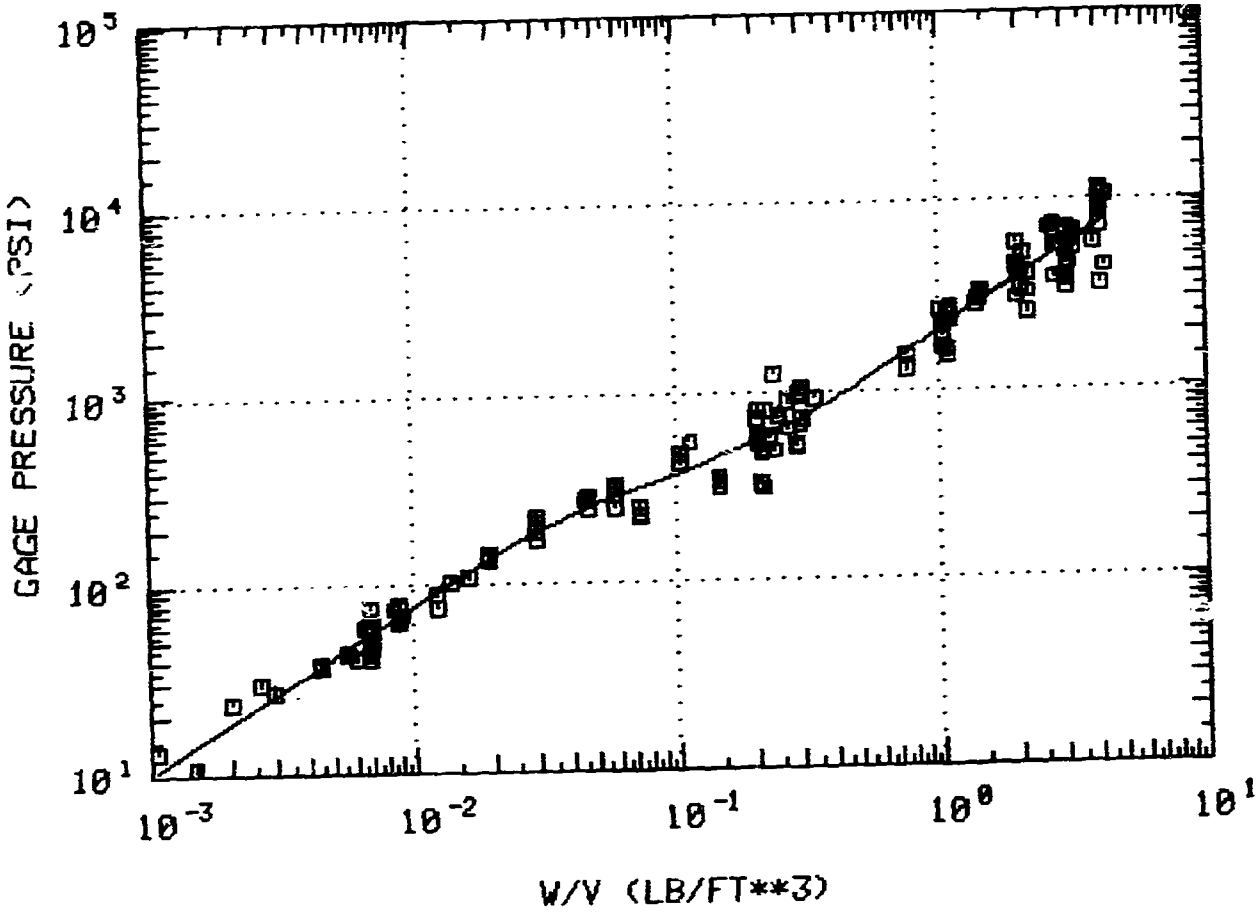

Figure 4. Peak Quasi-Static Pressure Versus the Ratio of Charge Weight to Enclosure Volume (Engineering Units)

$$\log p_{QS} = a_0 + a_1 \log (W/V) + a_2 [\log (W/V)]^2 + a_3 [\log (W/V)]^3 +$$

$$a_4 [\log (W/V)]^4 + a_5 [\log (W/V)]^5 + a_6 [\log (W/V)]^6 +$$

$$a_7 [\log (W/V)]^7 \qquad (23)$$

was then used to curve fit the entire range of data, where log represents the logarithm to the base 10. Such a high order polynomial is required because of the number of constraints: the slopes and intercepts at each end, the points where the polynomial connects with the straight lines, and the constraint that the curve be a least-squares fit. This is a total of seven constraints which stipulates at least a sixth-order polynomial for the curve fit. But the appearance of the data in Figure 3 implies that an odd function (as opposed to an even function) should be used. Hence, a seventh-order polynomial becomes the minimum order polynomial stipulated. Table 2 lists the coefficients of Equation (23) as well as the linear expressions for the two asymptotes. Table 3 lists the comparable coefficients and asymptotes for pressure in psi and W/V in lb/ft^3 (Figure 4).

The standard deviation for Equation (23) has also been computed but needs to be interpreted properly. The standard deviation, σ, is usually used as an estimate of the scatter in data, or error in predictions. One standard deviation encompasses approximately 68 percent of all data values. The uncertainty in estimating an observable is often written as the calculated quantity plus or minus one standard deviation:

$$\log p_{QS} = \log \hat{p}_{QS} \pm \sigma_c \qquad (24)$$

where p_{QS} is the estimated quasi-static pressure, $\hat{p}_{QS}$ is the computed quasi-static pressure from the curve fit, and σ_c is the computed standard deviation. Define σ_o such that

$$\log \sigma_o = \sigma_c \qquad (25)$$

The right-hand side of Equation (24) can then be written as

$$\log \hat{p}_{QS} \pm \log \sigma_o \qquad (26)$$

so that Equation (24) can be rewritten as:

Table 2. Summary of Peak p_{QS} Versus W/V

[MPa Versus kg/m^3]

$$\log \hat{p}_{QS} = 0.30759 + 0.51815 \log (W/V) - 0.150534 [\log (W/V)]^2 +$$

$$0.31892 [\log (W/V)]^3 + 0.10434 [\log (W/V)]^4 - 0.14138 [\log (W/V)]^5 +$$

$$- 0.019206 [\log (W/V)]^6 + 0.021486 [\log (W/V)]^7$$

Correlation Coefficient, r: 0.993

One Standard Deviation: $\sigma_o = 1.247$

$$\frac{\hat{p}_{QS}}{1.247} \leq p_{QS} \leq 1.247 \hat{p}_{QS}$$

Asymptotes:

$W/V \leq 0.4$ kg/m^3	$\hat{p}_{QS} = 2.347 (W/V)^{0.8395}$	$\sigma_o = 1.143$
$W/V \geq 11.0$ kg/m^3	$\hat{p}_{QS} = 1.1004 (W/V)^{0.9202}$	$\sigma_o = 1.300$

Table 3. Summary of Peak p_{QS} Versus W/V

[psi Versus lb/ft^3]

$$\log \hat{P}_{QS} = 3.3138 + 0.952133 \log (W/V) + -0.023074 [\log (W/V)]^2 +$$

$$- 0.317807 [\log (W/V)]^3 + 0.149364 [\log (W/V)]^4 + 0.374595 [\ln (W/V)]^5 +$$

$$0.161978 [\log (W/V)]^6 + 0.021486 [\log (W/V)]^7$$

Correlation Coefficient, r: 0.993

One Standard Deviation: $\sigma_o = 1.247$

$$\frac{\hat{P}_{QS}}{1.247} \leq p_{QS} \leq 1.247 \hat{P}_{QS}$$

Asymptotes:

$W/V \leq 0.025$ lb/ft^3	$\hat{P}_{QS} = 3495. (W/V)^{0.8435}$	$\sigma_o = 1.143$
$W/V \geq 0.70$ lb/ft^3	$\hat{P}_{QS} = 2049. (W/V)^{0.9393}$	$\sigma_o = 1.300$

$$\log\left(\hat{p}_{QS}/\sigma_o\right) \leq \log p_{QS} \leq \log\left(\sigma_o\, \hat{p}_{QS}\right) \tag{27}$$

$$\frac{\hat{p}_{QS}}{\sigma_o} \leq p_{QS} \leq \sigma_o\, \hat{p}_{QS} \tag{28}$$

Tables 2 and 3 give σ_o, as well as the correlation coefficient (which is a measure of the confidence of the curve fit).

Here we would like to mention our uncertainty of whether the slopes of the two asymptotes should have the same value. The slopes are not appreciably different, and particularly with the scatter prevelant for large W/V, it is not unreasonable to speculate that the slope should be identical. However, for the present, we have elected to report the linear least-squares, that is, the best fit to the data.

In deriving Equation (10), the assumption was made that the flow through the vent (for $\alpha_{eff} \neq 0$) is small relative to the rate of energy release so that the maximum quasi-static pressure occurs before significant venting has transpired. Keenan and Tancreto [22] obtained no measurable quasi-static pressure for values of $(\alpha_{eff}\, A/V^{2/3}) \geq 0.772$. Of the data plotted in Figures 3 and 4, the maximum reduced vent area ratio was 0.3246. Thus, Figures 3 or 4, and Tables 2 or 3, are valid for

$$0 \leq \frac{\alpha_{eff}\, A}{V^{2/3}} \leq 0.3246 \tag{29}$$

For a vented enclosure ($\alpha_{eff} \neq 0$), Equation (16) suggests that the duration, $\bar{t}$, be plotted versus the reduced pressure, $\bar{p}$, given by Equation (9). Seventy of the data points from Figure 3 or 4 represent vented enclosures, and these are plotted in Figure 5. It can be seen that the duration has considerable scatter because of the difficulty in determining when the overpressure has returned to ambient. Note, however, that the uncertainty in duration has negligible impact on the impulse since the total area under the pressure time curve is not sensitive to the exact location of t_{max}. A linear least-squares curve fit has been performed on the data and is shown in Figure 5, and the results are summarized in Table 4.

From the linear curve fit, it is straightforward to compute t_{max} from Equation (15) as a function of $\bar{p}$:

$$t_{max} = \frac{V}{a_o\, \alpha_{eff}\, A}\,(0.4284)\left(\frac{p_{QS} + p_o}{p_o}\right)^{0.3638} \tag{30}$$

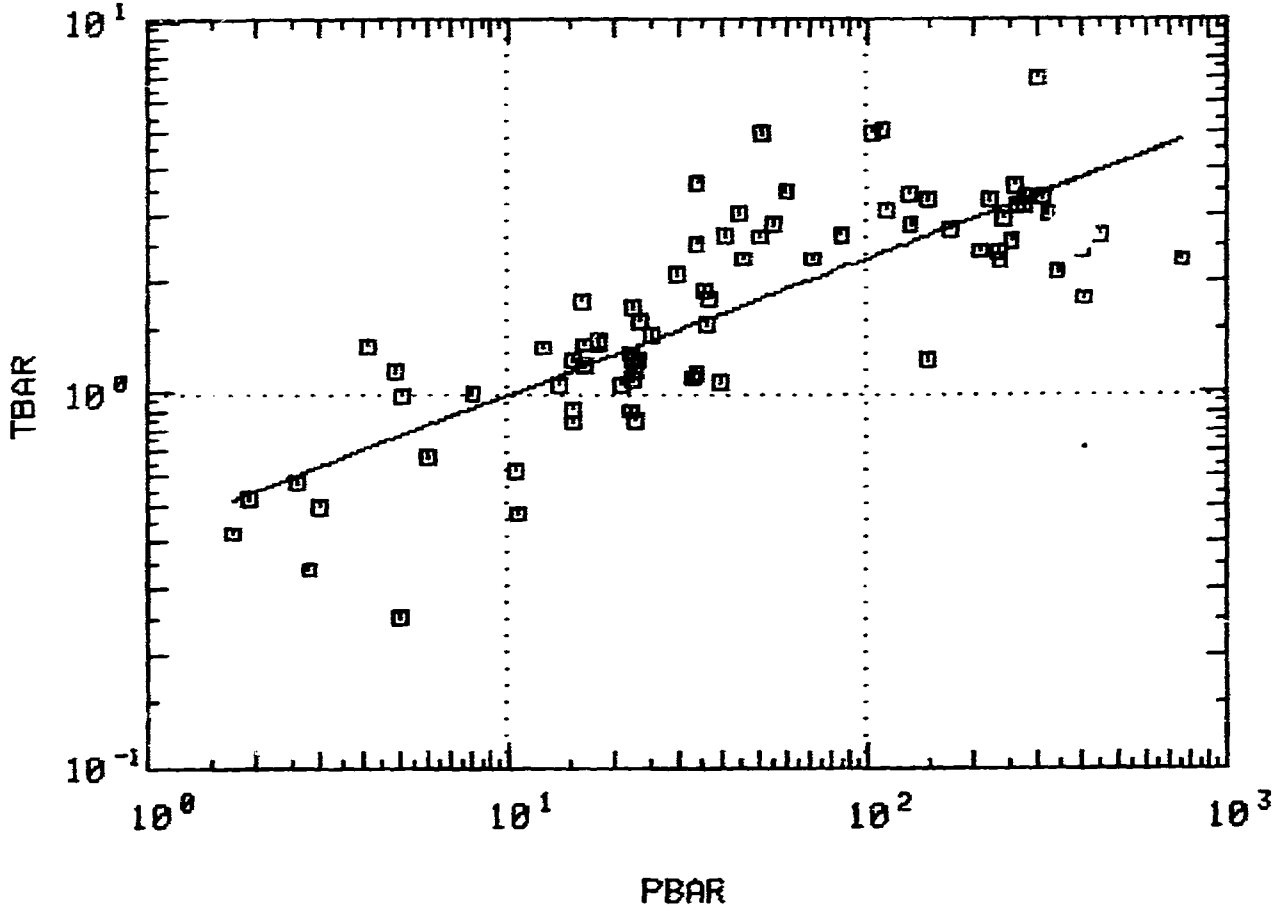

Figure 5. Reduced Duration Versus Reduced Pressure

Table 4. Summary of $\bar{\tau}$ Versus $\bar{p}$

$$\bar{\tau} = \frac{t\, a_o}{V^{1/3}} \quad \frac{a_{eff}\, A}{V^{2/3}}$$

$$\bar{p} = \frac{p_{QS} + p_o}{p_o}$$

Linear Curve Fit:

$$\hat{\bar{\tau}} = 0.4284\ (\bar{p})^{0.3638}$$

Correlation Coefficient, r: 0.799

One Standard Deviation: $\sigma_o = 1.50$

$$\frac{\hat{\bar{\tau}}}{1.50} \leq \bar{\tau} \leq 1.50\ \hat{\bar{\tau}}$$

The constant c in Equation (17) can now be evaluated:

$$p_o = (p_{QS} + p_o)\, e^{-c\, t_{max}} \tag{31}$$

$$c = \frac{1}{t_{max}} \ln\left(\frac{p_{QS} + p_o}{p_o}\right) \tag{32}$$

The specific impulse is then obtained from Equation (18), which after some rearrangement of terms, reduces to:

$$i_s = \left(\frac{p_{QS}}{\ln \bar{p}} - p_o\right) t_{max} \tag{33}$$

where $\bar{p}$ is given by Equation (9) and t_{max} is given by Equation (30).

As we have already stated, and just shown with Equation (33), the specific impulse can be obtained directly from the peak quasi-static pressure and the duration. However, because of the interest in specific impulse for computing the loading of structures, it is often convenient to have a graphical representation of specific impulse. Equation (20) indicates that an appropriate parameter for the abscissa is the reduced pressure. Sufficient information was reported to compute specific impulses for 75 of the tests. Figure 6 displays these reduced impulses, $\bar{i}_s$, versus the reduced pressure. A linear least-squares curve fit was also performed on these data, and is displayed in Figure 6. Table 5 summarizes the curve fitting information.

Quadratic least-squares curve fits were also performed on the data in Figures 5 and 6. However, the standard deviations differed by less than seven percent between the linear and quadratic curve fits for duration, and differed by only two percent for the reduced impulse. A two-sample comparison of variance was performed using the F ratio test at a 99 percent confidence level. For the linear and quadratic curve fits to be different statistically, the ratio of their respective σ's must exceed approximately 1.7. Since the ratio of their σ's is much less than 1.7, there is no significant difference in the linear versus quadratic curve fits -- hence, only the expressions for the linear curve fits have been reported.

SUMMARY

A sizeable quantity of data have been compiled and analyzed to obtain peak quasi-static pressure, and the duration and impulse for explosions within structures. Similitude analysis indicated an appropriate choice of parameters for graphically displaying the data. Peak quasi-static pressure was found to

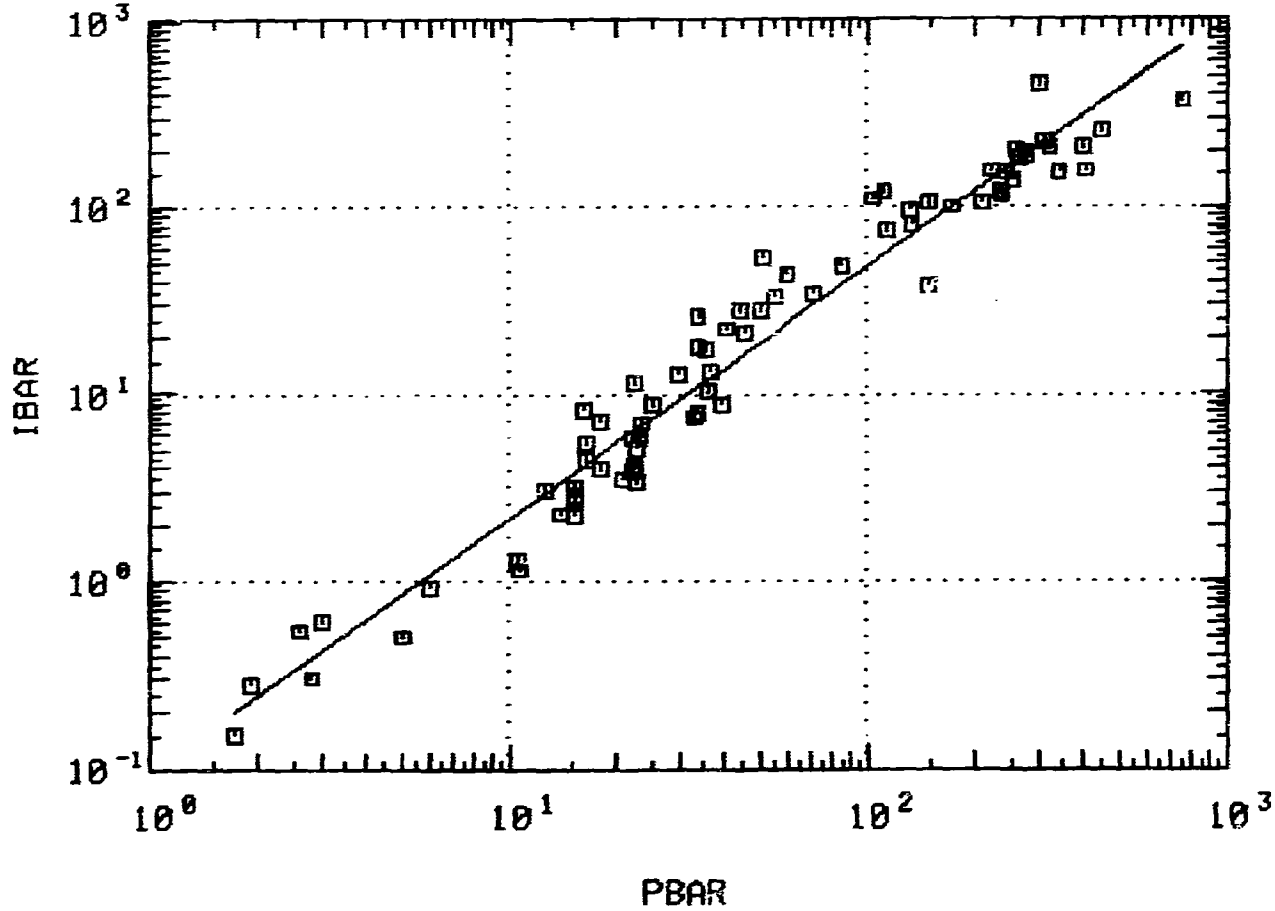

Figure 6. Reduced Specific Impulse Versus Reduced Pressure

Table 5. Summary of $\bar{i}_g$ Versus $\bar{p}$

$$\bar{i}_g = \frac{i_g \, a_o \, \alpha_{eff} \, A}{p_o \, V}$$

$$\bar{p} = \frac{p_{QS} + p_o}{p_o}$$

Linear Curve Fit:

$$\hat{i}_g = 0.0953 \, (\bar{p})^{1.351}$$

Correlation Coefficient, r: 0.977

One Standard Deviation: $\sigma_o = 1.53$

$$\frac{\hat{i}_g}{1.53} \leq \bar{i}_g \leq 1.53 \, \hat{i}_g$$

be a function of charge weight to chamber volume. Also, a nondimensional duration and a nondimensional specific impulse were found to be functions only of the reduced, i.e., nondimensional, pressure. The data range over several orders of magnitude and have thus been presented on log-log plots. Least-squares curve fits have been performed and reported, with their standard deviations, to provide appropriate analytic functions to relate the physical parameters. Thus, for high-order detonations within enclosures, the peak quasi-static pressure, and if the enclosure is vented, the duration and specific impulse, can be ascertained from the graphs on the respective analytic expressions.

ACKNOWLEDGEMENTS

The authors gratefully acknowledge the management of the Engineering Sciences Division of Southwest Research Institute who provided time and support for this research endeavor. Additionally, we would give special thanks to A. Jenssen of the Norwegian Defence Construction Service who graciously supplied a tremendous amount of the experimental data which have been analyzed and reported.

REFERENCES

1. Hans R. W. Weibull, "Pressures Recorded in Partially Closed Chambers at Explosion of TNT Charges," Annals of the New York Academy of Sciences, Volume 152, Article 1, October 1968, pp. 357-361.

2. C. N. Kingery, R. N. Schumacher, and W. O. Ewing, "Internal Pressures from Explosions in Suppressive Structures," BRL Memorandum Report ARBRL-MR-02848, USA Ballistic Research Laboratory, Aberdeen Proving Ground, Maryland, 1978.

3. J. F. Proctor and W. S. Filler, "A Computerized Technique for Blast Loads from Confined Explosions," Minutes of the 14th Annual Explosives Safety Seminar, New Orleans, Louisiana, 8-10 November 1972, pp. 99-124.

4. G. F. Kinney and R. G. S. Sewell, "Venting of Explosions," NWC Technical Memorandum 2448, Naval Weapons Center, China Lake, California, 1974.

5. R. N. Schumacher, C. N. Kingery, and W. O. Ewing, "Airblast and Structural Response Testing of a 1/4 Scale Category 1 Suppressive Shield," BRL Memorandum Report No. 2623, USA Ballistic Research Laboratory, Aberdeen Proving Ground, Maryland, 1976.

6. D. M. Koger and G. L. McKown, "Category 5 Suppressive Shield (TDP)," Report EM-TR-76001, Headquarters, Edgewood Arsenal, Aberdeen Proving Ground, Maryland, 1975.

7. E. D. Esparza and A. B. Wenzel, "Development of a Blast Simulator for Testing Simulated Aircraft Fuel Tanks," ITCG/AS-76-T-004, Naval Air Systems Command, Washington, D.C., 1978.

8. E. D. Esparza, W. E. Baker, and G. A. Oldham, "Blast Pressures Inside and Outside Suppressive Structures," Report EM-CR-76042, Headquarters, Edgewood Arsenal, Aberdeen Proving Ground, Maryland, 1975.

9. S. Zilliacus, W. E. Phyillaier, and P. K. Shorrow, "The Response of Clamped Circular Plates to Confined Explosive Loadings," Report No. 3987, Naval Ship Research and Development Center, Bethesda, Maryland, 1974.

10. J. F. Proctor, "Internal Blast Damage Mechanisms Computer Program," JTCG/ME-73-3, Air Force Systems Command, Wright-Patterson AFB, Ohio, 1973.

11. A. Skjeltorp, T. Hegdahl, and A. Jenssen, "Underground Ammunition Storage, Report I: Test Programme, Instrumentation, and Data Reduction," Norwegian Defence Construction Service, Oslo, Norway, 1975.

12. A. Skjeltorp, T. Hegdahl, and A. Jenssen, "Underground Ammunition Storage: Model Tests to Determine Air Blast Propagation from Accidental Explosions," Nr 59/70, Norwegian Defence Construction Service, Oslo, Norway, 1970.

13. A. Skjeltorp, T. Hegdahl, and A. Jenssen, "Underground Ammunition Storage: Blast Propagation in the Tunnel System. Report IIA: Chamber Pressure," Nr 79/72, Norwegian Defence Construction Service, Oslo, Norway, 1975.

14. A. Skjeltorp, T. Hegdahl, and A. Jenssen, "Underground Ammunition Storage: Blast Propagation in the Tunnel System. Report IIIA: Single Chamber Storage, Variable Tunnel Diameter and Variable Chamber Volume," Nr 81/72, Norwegian Defence Construction Service, Oslo, Norway, 1975.

15. A. Skjeltorp, T. Hegdahl, and A. Jenssen, "Underground Ammunition Storage: Blast Pressure in the Tunnel System. Report III: Single Chamber Storage, Variable Tunnel Diameter and Variable Chamber Volume," Nr 81/72, Norwegian Defence Construction Service, Oslo, Norway, 1972.

16. A. Skjeltorp, T. Hegdahl, and A. Jenssen, "Underground Ammunition Storage. Model Test to Investigate the Strength and Effectiveness of a Self-Closing Concrete Block, Test IV," Nr 85/72, Norwegian Defence Construction Service, Oslo, Norway, 1972.

17. A. Skjeltorp, T. Hegdahl, and A. Jenssen, "Underground Ammunition Storage. Model Test to Investigate the Strength and Effectiveness of a Self-Closing Concrete Block, Test V," Nr 98/74, Norwegian Defence Construction Service, Oslo, Norway, 1973.

18. A. Skjeltorp, T. Hegdahl, and A. Jenssen, "Underground Ammunition Storage: Blast Propagation in the Tunnel System. Report IVA: Connected Chamber Storage, Variable Chamber Volume and Variable Angle Between Branch and Main Passageway," Nr 82/72, Norwegian Defence Construction Service, Oslo, Norway, 1975.

19. A. Skjeltorp, T. Hegdahl, and A. Jenssen, "Underground Ammunition Storage: Blast Propagation in the Tunnel System. Report IV: Connected Chamber Storage, Variable Chamber Volume amd Variable Angle Between Branch and Main Passageway," Nr 82/72, Norwegian Defence Construction Service, Oslo, Norway, 1972.

20. J. C. Hokanson, E. D. Esparza, W. E. Baker, and N. R. Sandoval, "Determination of Blast Loads in the Damage Weapons Facility, Volume 1, Phase 1," SwRI Report 6578-101, Mason and Hanger-Silas Mason Company, Inc., Amarillo, Texas, 1982.

21. J. C. Hokanson, E. D. Esparza, W. E. Baker, N. R. Sandoval, and C. E. Anderson, "Determination of Blast Loads in the Damage Weapons Facility, Volume 1, Phase 2," SwRI Report 6578-102, Mason and Hanger-Silas Mason Company, Inc., Amarillo, Texas, 1982.

22. W. A. Keenan and J. E. Tancreto, "Blast Environment from Fully and Partially Vented Explosions in Cubicles," Technical Report 51-027, Civil Engineering Laoratory, Naval Construction Battalion Center, Port Hueneme, California, 1974.

23. J. A. Owczarek, Fundamentals of Gas Dynamics, International Textbook Company, Scranton, Pennsylvania, 1964.

24. W. E. Baker and G. A. Oldham, "Estimates of Blow-Down of Quasi-Static Pressures in Vented Chambers," Edgewood Arsenal Contractor Report EM-CR-76029, Report No. 2, Edgewood Arsenal, Aberdeen Proving Ground, Maryland, 1975.

25. W. E. Baker, P. A. Cox, P. S. Westine, J. J. Kulesz, and R. A. Strehlow, Explosion Hazards and Evaluation, Elsevier Scientific Publishing Company, Amsterdam, 1982.